Visual Neuroscience (1998), **15**, 333–348. Printed in the USA.

The selective impairment of the perception of first-order motion by unilateral cortical brain damage

LUCIA M. VAINA,[1,2] NIKOS MAKRIS,[3] DAVID KENNEDY,[1,2,3] AND ALAN COWEY[4]

[1]Boston University, Departments of Biomedical Engineering and Neurology, Brain and Vision Research Laboratory, Boston
[2]Harvard Medical School, Department of Neurology, Brigham and Women's Hospital, Boston
[3]Center for Morphometric Analysis, Massachusetts General Hospital, Charlestown
[4]University of Oxford, Department of Experimental Psychology, Oxford, U.K.

(RECEIVED April 7, 1997; ACCEPTED September 23, 1997)

Abstract

First-order (Fourier) motion consists of stable spatiotemporal luminance variations. Second-order (non-Fourier) motion consists instead of spatiotemporal modulation of contrast, flicker, or spatial frequency. In spite of extensive psychophysical and computational analysis of the nature and relationship of these two types of motion, it remains unclear whether they are detected by the same mechanism or whether separate mechanisms are involved. Here we report the selective impairment of first-order motion, on a range of local and global motion tasks, in the contralateral visual hemifield of a patient with unilateral brain damage centered on putative visual areas V2 and V3 in the medial part of the occipital lobe. His perception of second-order motion was unimpaired. As his disorder is the obverse of that reported after damage in the vicinity of human visual area MT (V5), the results support models of motion processing in which first- and second-order motion are, at least in part, computed separately at the extrastriate cortical level.

Keywords: First-order motion, Second-order motion, Visual cortex, Psychophysics, Neuroimaging

Introduction

We can usually perceive the direction of visual motion by low-level mechanisms which perform spatiotemporal correlations of the raw luminance values in the visual field. Several such mechanisms have been formulated (Reichardt, 1961; Marr & Ullman, 1981; van Santen & Sperling, 1985; Watson & Ahumada, 1985) and although they differ, all assume that the ability to detect motion is predictable from the spatiotemporal Fourier power spectrum of the stimulus. Models of this type are referred to as performing standard motion analysis (Chubb & Sperling, 1988, 1989), Fourier, or first-order motion analysis. However, psychophysical experiments demonstrate that we can perceive direction of motion when the definitional cues used in models of standard motion analysis are uninformative (Ramachandran et al., 1973; Pantle & Picciano, 1976; Sperling, 1976; Petersik et al., 1978; Pantle & Turano, 1986; Green, 1986; Chubb & Sperling, 1988, 1989; Cavanagh & Mather, 1989; Turano & Pantle, 1989; Victor & Conte, 1990; Wilson et al., 1992; Derrington et al., 1993; Smith et al., 1994) and the terms non-Fourier and second-order motion were therefore introduced to describe stimuli which have no overall directional component in the Fourier domain. In such stimuli, what moves is not particular luminance contrast but modulation of other stimulus attributes, such as contrast, flicker, or spatial frequency.

It is possible that from the outset the visual system uses different methods for analyzing first- and second-order motion. Thus, second-order motion may be mediated by a high-level feature matching mechanism, reminiscent of the long-range system proposed by Braddick (1974), or by a postattentive tracking mechanism suggested by Cavanagh (1990). While there is psychophysical evidence for the feature-based theory for discriminating direction in second-order motion stimuli, there is also evidence that second-order motion is not primarily detected by a high-level, feature-based mechanism (Georgeson & Harris, 1990).

Alternatively, there are several models which propose that extraction of motion from second-order stimuli involves some grossly nonlinear transformation of stimulus luminance, such as a simple rectification or squaring of local stimulus contrast, before applying standard motion analysis (Chubb & Sperling, 1988, 1989; Turano & Pantle, 1989; Wilson et al., 1992). Common to these models is that first- and second-order motion are detected by different low-level mechanisms which nonetheless operate on qualitatively similar principles. The basic hypothesis is that second-order motion can indeed be detected with standard oriented motion energy detectors after a nonlinear transformation has been applied to the band-pass spatial-frequency filtered image. Other models (Johnston et al., 1992; Grzywacz et al., 1995) propose that first- and second-order motion are detected by a single, low-level mechanism.

Reprint requests to: Lucia M. Vaina, Boston University, Brain and Vision Research Laboratory, Department of Biomedical Engineering, 44 Cummington Street, Boston, MA 02215, USA.

Few physiological studies address both first- and second-order motion. Albright (1992) reported that directionally selective neurons in area MT are indifferent to the attributes that define the motion, i.e. they are invariant across both luminance and contrast cues. O'Keefe et al. (1993) and O'Keefe & Movshon (1996) described results from monkey STS (superior temporal sulcus) that responded to *both* first- and second-order motion stimuli (where second-order motion was defined by contrast cues). Zhou and Baker (1993) showed that cells in primary visual cortex of cats respond selectively to the direction of moving contrast-modulated gratings (second-order), suggesting that the motion of the contrast "envelope" is computed by low-level mechanisms. The few existing physiological studies have not yet provided definitive evidence for selectivity specific to second-order motion, but they indicate that neurons in several areas along the "dorsal" processing stream respond to second-order motion.

In contrast to the paucity of physiological studies addressing first- and second-order motion, a wealth of psychophysical studies involving a variety of stimulus types reinforces the hypothesis that first- and second-order motion might be encoded by distinct low-level mechanisms (e.g. Derrington & Badcock, 1985; Boulton & Baker, 1991, 1993; Mather & West, 1993; Ledgeway & Smith, 1994; Holliday & Anderson, 1994). If they operate in parallel rather than in sequence, they might be grossly spatially segregated at some cortical level and hence dissociable by different cortical lesions. Indeed, such a demonstration would provide unequivocal evidence for two separate mechanisms mediating first- and second-order motion.

There is evidence that second-order motion can be selectively impaired in the contralateral visual hemifield following unilateral cortical damage to extrastriate visual cortex. Thus, Plant et al. (1993) demonstrated this in three patients by showing that contrast thresholds for discriminating the direction of motion of a contrast-modulated grating (a second-order motion stimulus) were elevated in the hemifield contralateral to the lesion even though the discrimination threshold for a similar task involving a luminance modulated grating was not impaired. Using a variety of first- and second-order psychophysical tasks of both local and global motion, Vaina and coworkers (Vaina et al., 1993; Vaina & Cowey, 1996) demonstrated a selective impairment of second-order motion in the contralateral hemifield of a patient with small cortical lesion just dorsal to the presumed area MT (V5) of the human brain. Here we present the first demonstration of the complementary disturbance: a neurological patient, RA, showed a selective impairment of first-order motion perception following a restricted unilateral lesion close to the medial surface of the occipital lobe, just above the calcarine fissure and involving what are probably parts of cortical areas V2 and V3.

Since we were interested in the specificity of RA's disorder, the paper presents first his performance on static tasks, followed by the results on a range of typical first-order motion tasks such as speed, direction, and two-dimensional (2-D) form discrimination, and a second-order motion task which was also used in physiological studies in monkeys (Albright 1992; O'Keefe et al., 1993; O'Keefe & Movshon, 1996). Finally we present RA's performance on tests that directly compare the two types of motion perception, using tasks that are otherwise similar. Where possible the patient was tested within a few weeks of his stroke and again after about 18 months in order to see whether his recovering visual performance occurred across all tasks on which he was initially impaired.

Some of this work was presented at the annual meeting of the Society of Neurosciences (Vaina & Cowey, 1996) and at the Second Human Brain Mapping Conference (Vaina et al., 1996).

In this study, we first provide a detailed clinical neurological and neuropsychological background on RA and a detailed analysis of the anatomical locus of his lesion (see Methods). In Section A in Results, we report RA's normal performance on psychophysical discrimination tasks of static forms, orientation, and spatial relations. Section B provides the results from testing RA's ability to discriminate speed, direction, and two-dimensional shape generated by differences in speed and direction of motion. It also presents the surprising result that, in spite of RA's impaired performance on these motion tasks (when presented in the visual field contralateral to the lesion), he was normal on a task of direction discrimination with a second-order motion stimulus (in both visual fields). This motivated our detailed investigation of RA's performance on several first- and second-order motion tasks (Section C in Results).

Methods

The patient: Background

The experiments were carried out on a neurological patient RA, and a variable number of control subjects of similar age and education but with normal vision. RA is a right-handed retired computer manager who suffered a right hemisphere CVA in January 1994 at the age of 66. For 3 weeks, he had slurred speech and weakness of the left arm and, less evidently, the leg. He also complained of a "terrific headache" at the back of his head on the right side. His medical history included coronary artery disease, diabetes mellitus, hypertension, and hypercholesterolemia. On initial neurological examination he had abnormal sensation in his left arm and leg. CT scan and carotid ultrasound obtained on the day of the stroke were normal, suggesting that his CVA might have been caused by an embolic event. He was admitted to a rehabilitation hospital for treatment of his left-sided weakness. He reported that after his stroke, while a passenger in a car, he could no longer reliably judge the speed or direction of other moving vehicles. Looking at the clock on the wall, he said that he could not see between the 7 and 10 on it, and thus he felt that there was a "hole" in his vision. He and his family reported that after the incident he could not adequately monitor the visual space around him. To quantify his cognitive and perceptual abilities, we carried out both neuropsychological and visual-perceptual evaluations. Informed consent was obtained from the patient and the normal control subjects according to the requirements of Boston University Human Subjects' Committee.

Neuropsychological evaluation

Using the Wechsler Adult Scale Revised test (WAIS-R) for general verbal and performance abilities, RA scored in the average range, Verbal IQ = 92 and Performance IQ = 92. His vocabulary and basic language skills were normal. Copying and drawing of simple two-dimensional figures were normal, as were his constructional skills (tested with the Block assembly test of the WAIS-R). On the Wechsler Memory Scale, his immediate recall of five simple figures was excellent, whereas he recalled only a few fragments of these figures after 30 min. This was in contrast with his excellent spatial memory. On a subset of tests from the Visual Object and Space Perception neuropsychological battery (Warrington & James, 1991), his scores were normal on the number location test for spatial localization, the shape-detection screening test, and the recognition of incomplete letters. However, he was impaired on the silhouette test (portrayed in a noncanonical view) which assesses

object recognition from incomplete information, e.g. some of the key characteristics/features are not visible in a noncanonical view. Although he correctly categorized the silhouettes of a pig, cow, sheep, duck, or seal as animals or birds, he could not identify them individually. He totally failed to identify most of the man-made objects shown, perhaps because they have less salient features than do animals. For example, he identified the silhouettes of "a corkscrew" as a "vase," "glasses" as "some animal, with a long beak," "scissors" as "bird," and a "pick axe" as "bird that pokes its beak in the sand." He correctly identified very familiar things like a cup, tractor, shoe, binoculars, or ladder.

His static contrast sensitivity, assessed with the Pelli-Robson chart (Metropia Ltd., 1988), was normal for each eye. He also had normal performance on a computer-controlled test for assessing contrast sensitivity for both detection and discrimination of static and moving sinusoidal gratings ranging in spatial frequency from 0.2 cycle/deg to 5 cycles/deg. In this test, the stimuli were presented separately to each eye and in each visual field (left and right). In all cases, he scored within normal limits as compared with age-matched control subjects. Color vision tested with the Farnsworth-Munsell-100 hue test (Farnsworth, 1943) and with the isochromatic plates (Ichikawa et al., 1983) was normal. Stereovision tested with the Randot clinical test (Randot Stereotest, 1956) was informative because, while he could correctly discriminate the apparent depth generated by disparity, he was unable to identify any of the simple shapes shown. For example, he identified the "triangle" as a "pitcher," the "star" as a "teddy bear," and the letter "E" as a "baby face." This was in contrast with his normal recognition of complete two-dimensional drawings of common objects presented in canonical views (from the Boston Naming test) and of incomplete letters (from the VOSP battery).

Neuroophthalmological and neuroimaging assessments

In March 1994, one month after his discharge from the rehabilitation hospital, RA received quantitative assessment of his vision and visual fields and had MRI (magnetic resonance images) studies of his brain for determining the extent and etiology of his lesion.

Neuroophthalmological assessment

Visual acuity was 20/20 in each eye with myopic spectacle correction. Intraocular pressures were normal and the pupils reacted briskly. He had full extraocular muscle function when tracking movement, and saccades to targets within his intact field were normal. He had normal optokinetic responses to striped drum rotations up, down, left, and right and normal vestibulo-ocular reflex.

Visual fields were examined by two techniques. The Goldmann visual field was obtained using test spots I4e, I3e, and I2e. The I2e test spot correlated best with the Humphrey visual-field test using the 24-2 program. Both tests showed a left inferior quadrantanopia. In the left eye, the visual-field defect extended slightly into the upper quadrant. This scotoma resolved and 16 months after the lesion RA recovered full-field vision (formally assessed by perimetry every 2–3 months). After the latter evaluation, we repeated many of the initial tests of motion perception and, as a result of their outcome, carried out the comparison of performance on first-order and second-order motion.

MRI and morphometric analysis

Magnetic resonance images were obtained with a 1.5-Tesla GE Signa System (General Electric Medical Systems) using our standard protocol for obtaining three-dimensional (3-D) reconstruction of the images. No intravenous contrast was administered. Saggital T1-weighted axial proton density and T2-weighted images (3 mm thick, no gap) were first obtained without contrast, followed by additional thinner coronal SPGR images (1.5 mm thick, no gap). Imaging parameters were FOV 24 cm, interleaved acquisition, TR 3000 ms, and Te 80 ms. The first echo was acquired with a Te of 30 ms proton sensitivity weighted image. Data acquired in 3-D raster metrics (SD Fourier transform spoiled gradient-recalled acquisition in steady state) were stored in coronal images. The MRI indicated an infarction involving primarily grey matter in the medial territory of the posterior cerebral artery. On the MRI, it appeared as an area of abnormal signal intensity (T2 hyperintensity) at the occipital pole (Fig. 1) which extended rostrally above the calcarine fissure to a point about halfway along it. A smaller infarction was also present below the calcarine fissure. The abnormal area measured about 3 cm at its maximum dorso-ventral extent and about 2 cm in width at its widest. A small T2 hyperintensity was also noted within the right middle cerebral peduncle as well as in the pons and within the right thalamus, consistent with prior very small lacunar infarctions.

Lesion analysis

To optimize the criteria for delimiting anatomical structures across multiple scans, the volumetric image data were positionally normalized. Therefore, the MRI data set were reformatted and resliced in a new coordinate system, which has as its origin the midpoint of the anterior commissure-posterior commissure line (Talairach & Tournoux, 1988; Kennedy et al., 1987; Kennedy et al., 1989). These images were segmented using an algorithm which utilizes absolute and differential intensity contour mapping.

The lesion was mapped onto anatomical regions of interest (ROIs) based on a parcellation system that identifies "limiting fissures" and "limiting coronal planes" in order to provide complete boundaries for each region of interest (Rademacher et al., 1992). The system yields 46 parcellation units (PUs) in the cerebral cortex based on macrostructural correlates of functional anatomy and microstructural organization of the human cerebral cortex. Specifically, in the occipital lobe there are nine PUs: occipital pole (OP), lingual gyrus (LG), cuneus (CN), superior occipital lateral gyri (OLs), inferior occipital lateral gyri (OLi), occipital portion of the fusiform gyrus (OF), temporooccipital fusiform gyrus (TOF), middle temporal gyrus/temporo-occipital part (TO2), and inferior temporal gyrus/temporo-occipital part (TO3). Among them, parcellation units OP, CN, and LG are defined as follows: OP is delimited by the coronal plane set at the caudal tip of the cuneal fissure and, caudal to that plane, the cerebral hemispheric margins; CN is delimited by the parietooccipital fissure, the calcarine fissure, and the cerebral hemispheric margin; and LG is delimited by the collateral fissure, the calcarine fissure, and two coronal planes, i.e. one at the level of the rostral end of the calcarine fissure, and one at the level of the caudal end of the cuneal fissure.

The cortical lesion (Fig. 1, bottom) involved three PUs in the right occipital lobe: a portion of the caudal and medial part of the cuneus (CN), a portion of the superior and caudal part of the lingual gyrus (LG), and a portion of the most rostral and medial part of the occipital pole (OP).

Visual-perception tests

Patient RA had experienced problems with judging motion in everyday life. Yet his lesion is small and medial in the occipital lobe,

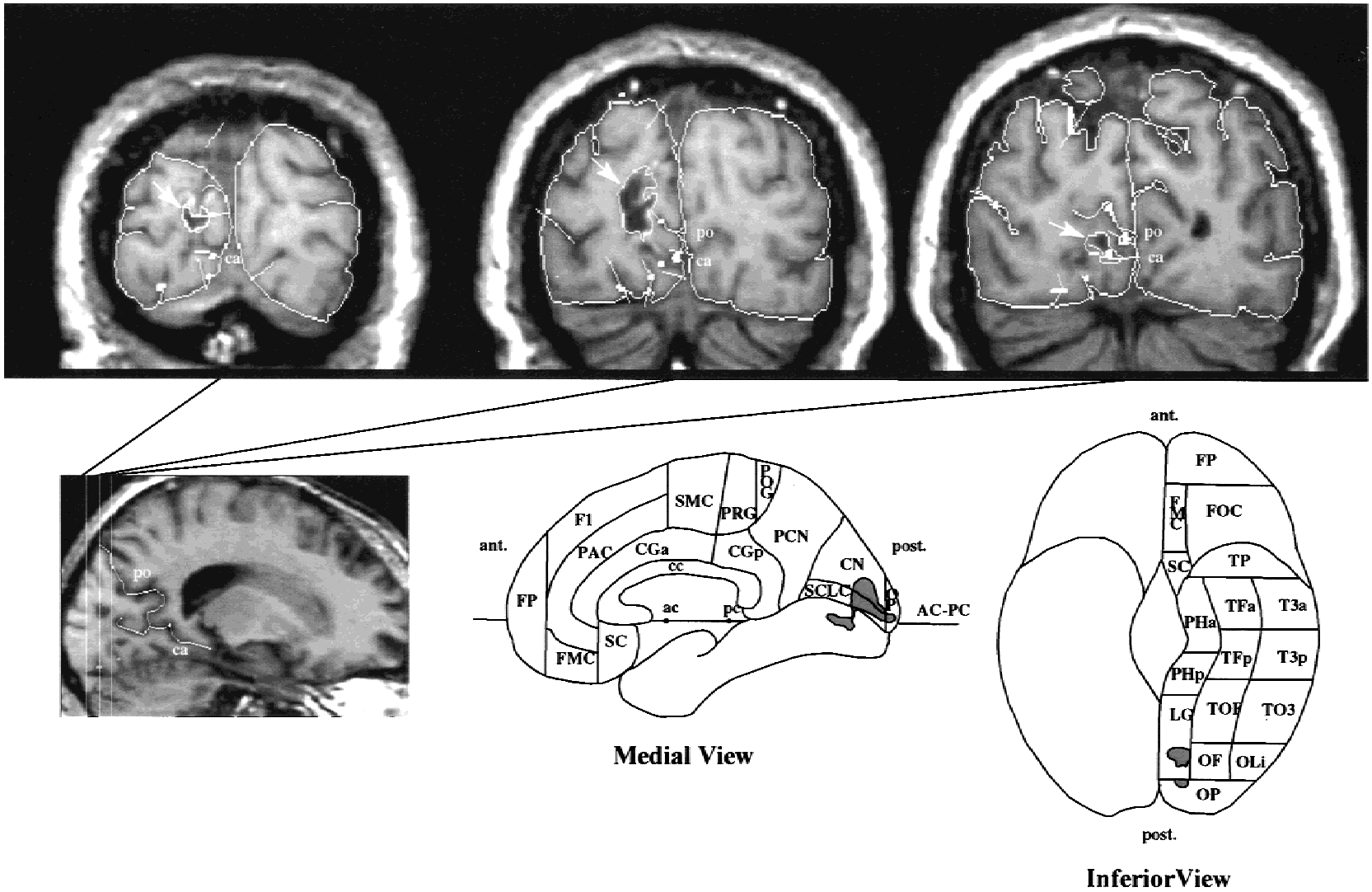

Fig. 1. Anatomic localization of infarct with cortical parcellation system. Top row: Three representative coronal slices spanning the region of the infarct. The locations of these images are shown in the sagittal image in the bottom row, left. Within each coronal image, the region of infarct is outlined (arrow). The sulcal identification was made using a cross-referential visualization system. The lesion in the right hemisphere appears on the left in each section and is adjacent to what appears to be an enlarged lateral ventricle. The white lines show the outlines and borders of the cortical parcellation units described in the text. Calcarine (ca) and parieto-occipital (po) sulci are indicated. Bottom row, middle and right: The localization of the infarct relative to the complete cortical parcellation system of Rademacher et al. (1992). The lesion intersects cortex of the CALC, SCLC, LG, and OP cortical parcellation units.

remote from the MT/V5 complex that has been associated with motion perception on the basis of neuropsychological (Zihl et al., 1983, 1991), psychophysical (Hess et al., 1989; Vaina et al., 1990*a*,*b*; Baker et al., 1991), and neuroimaging investigations (Zeki et al., 1991; Barbur et al., 1993; Watson et al., 1993; Tootell et al., 1995). It was also remote from the lateral lesion, adjacent and dorsal to area MT/V5, of patient F.D., whose perceptual disorder was specific for second-order motion (Vaina & Cowey, 1996). We therefore tested RA on a range of psychophysical tasks involving both stationary and moving stimuli, in order to characterize his disorder and to determine whether it was specific to motion and, if so, whether it involved a dissociation between first-order and second-order motion. With the tasks on which he was initially impaired, he was tested repeatedly at frequent intervals (1 to 3 weeks) for a period of 2 years. The results are reported as RA-I and RA-II, in which RA-II shows his performance after his recovery from the left inferior quadrantopia. The results reported as RA-I were obtained at least 6 months after his stroke.

General methods and procedures

All stimuli were generated and presented, and responses collected and analyzed using a Macintosh Quadra 650 computer with 16 MB RAM. Except for Experiment 6, stimuli were presented in the center of a color monitor (Apple Trinitron 0.25 mm pitch, 13-inch; 640 × 480 pixels; active viewing area 235 × 176 mm; vertical scanning frequency, 66.7 Hz and P22 phosphor). The system had 8 bits/gun pixel quality. The stimuli in Experiment 6 were displayed on a SuperMac Gray Scale 21-inch noninterlaced monitor (resolution 1152 × 870 pixels, active video display area 381–285 mm, page-white phosphor, vertical scanning frequency, 75 Hz). In Experiments 5–8, the stimuli were generated using a color table of 256 gray levels. The monitors were calibrated using VideoToolbox software (Pelli, 1995), and prior to each experimental session the internal *z*-axis linearization of the monitors was confirmed with a Minolta LC-1500 for the range of contrasts used.

Each motion display was generated by a rapid sequence of static exposures. Unless otherwise stated in the description of the experiment, each exposure lasted 45 ms (three videoframes) and was replaced by the next one in the next refresh, and stimuli were displayed for 22 exposures (1 s). Response time was unlimited and every 15–20 min, or as needed, the subjects took a short break. All the experiments took place in a quiet dark room, in which the only source of illumination came from the monitor. In the background examinations with a wide variety of first-order motion stimuli, unless specified in the test description, the space-average luminance of the stimuli was roughly 0.51 cd/m^2 for the sparse random dot patterns (2 dot/deg^2), 46.7 cd/m^2 for the dense random dot patterns (50% black and 50% white pixels), and 0.23 cd/m^2 for the surrounding screen background. Before beginning a test, subjects first adapted for 5 min to the dark condition, and all testing was preceded by practice trials of a wide range of difficulty which ensured that subjects understood the task. Only in the practice trials was feedback given to the subject (audible tone). Between trials, subjects viewed the screen that was a uniform mean luminance, except for the bright fixation mark. Except for the Efron Shapes test and Experiments 6 and 8 in which we used the method of constant stimuli, an adaptive staircase procedure began after the practice trials. The full range of steps in the adaptive staircase spanned 32 log units per decade.To minimize the number of trials in a single run, the staircase had two parts: the first consisted of three steps down until the first error followed by nine steps up until the next correct response, then two steps down until the next error followed by six steps up until the next correct response. The second part was a classic staircase, three consecutive correct responses, one step down, one error, one step up. (For details and comparisons with different staircase algorithms, see Saiviroporoon, 1992). The staircase was continued until 10 reversals had occurred. Threshold for each run was computed as the arithmetic mean of the last six reversals (the first four were disregarded), and the threshold for each stimulus was taken as the arithmetic mean of the thresholds from two runs.

Unless otherwise stated, subjects sat 60 cm from the screen and fixated a small black fixation mark at eye-level, 2 deg to the left or right of the imaginary margin of the display. All the experiments were done with binocular viewing. Subject's responses were verbal and the examiner entered them on the computer.

The results from RA and appropriate normal control subjects are plotted for each experiment. All the data for RA are the means of two threshold measurements obtained in the same experimental session. Filled circles show the data from stimuli presented in his normal right visual field and unfilled circles show the results from his left visual field contralateral to the right hemisphere lesion. (Exception to this rule are the data from Experiment 8 which was presented with central fixation, and the Efron Shape task in which data from presentation in the right and left visual field are combined because both RA and controls had almost perfect score.)

Results

A: Discrimination of static forms, orientation, and spatial relations

Since all the initial neuropsychological perceptual evaluations used pencil and paper tests and were shown with free viewing, we determined RA's perceptual abilities for stationary stimuli presented in each hemifield separately, using computer controlled displays. Figs. 2A–2D give a schematic view of the four types of display and the data from RA and control subjects. In *panel A*, the *Efron Shape* test (Efron, 1968), RA was presented on each trial with a shape and asked to judge whether it was a square or an oblong. The square subtended 5 deg × 5 deg and the oblongs subtended 5.25 deg × 4.77 deg, 4.6 deg × 5.5 deg, or 6.5 deg × 4 deg. For each of these dimensions 20 trials were presented, each for 0.5 s, in pseudorandom order. *Panel B* portrays the task of *degraded letters*. On each trial the subject had to identify the letter displayed for 0.5 s in the center of the display and surrounded by a static random pixel dot field of 50% density of black and white pixels. Static masking noise (like that of the background) superimposed on the letter was systematically titrated using the adaptive staircase procedure (from 0% noise, resulting in a white letter displayed in the dense random-dot background, to 100% noise in which the letter is indistinguishable from the background). *Panel C* shows the *spatial relations* test. This is a two-temporal alternatives forced-choice task (2TAFC). In the first frame a vertical bar (2 deg high), the referent, displayed on a sparse random-dot background pattern 10 deg in diameter and dot density 2 dots/deg^2 is flashed for 100 ms, followed by a blank screen (30 ms) and by a second frame identical in all respects to the first frame except that the bar's position is displaced left or right. Subjects are asked to report whether the vertical bar in the second frame was to the left or to the right of the referent bar. Threshold for discrimination-minimum-position difference is obtained using the staircase procedure to titrate the spatial position difference between the bar in

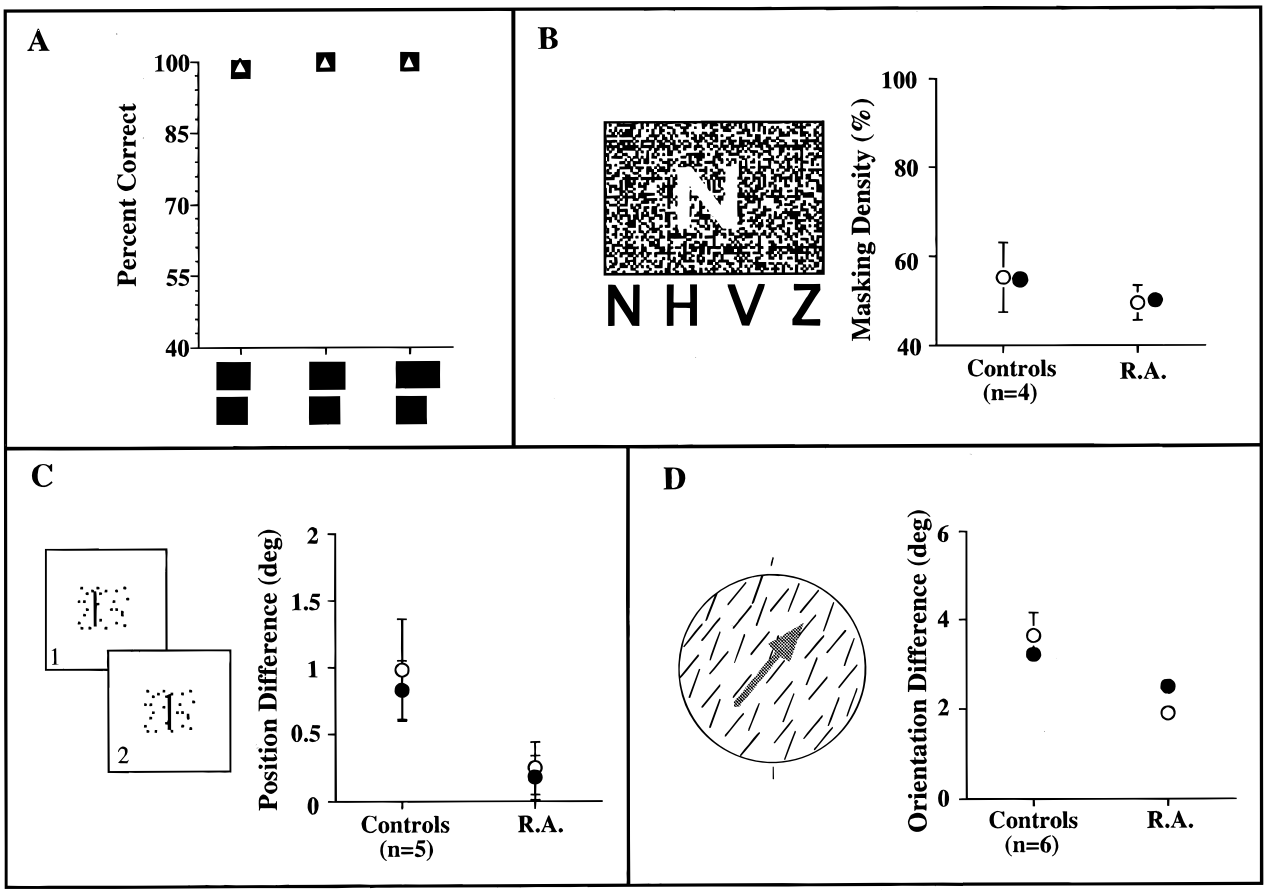

Fig. 2. The performance of patient RA and control subjects on the four tests involving static displays. In the shape-discrimination task (A), the performance of RA is indicated by triangles and was indistinguishable from that of 65 control subjects, indicated by black squares. As there were no differences between performance in the left and right hemifields, the results have been combined. B–D show the performance of RA and control subjects on tests of shape, position, and orientation discrimination, respectively. RA was as good or better than the normal controls in both his left and right hemifields.

the first and second frame. *Panel D* shows a schematic view of the display for *orientation discrimination*. The display, 10 deg in diameter, consists of short white lines, 2 arcmin wide and 4 arcmin core length value ± a jitter. Lines are positioned pseudorandomly within the aperture, with a constant density of 2 lines/deg^2. The global orientation of the lines is a variable angle to the left or right of true vertical, indicated by two short and clearly visible lines placed 0.5 deg above and below the display. In a 2AFC procedure, subjects are asked to determine whether the global orientation of the lines is to the right or the left with respect to true vertical. Threshold represents the smallest global orientation discriminated.

Figs. 2A–2D show RA's performance for stimuli presented in either the left or the right visual field, on the four types of discrimination involving static shapes. He was not impaired on any of these tasks when performance in his impaired field was compared either with that in the normal hemifield or with that of control subjects in each of their hemifields. His performance was superior to that of control subjects on some tasks, a pattern also seen on some motion tasks. We attribute this to his more extensive psychophysical experience than that of almost every control subject.

B: Visual motion perception

Since RA mentioned that he had trouble in perceiving movement on his left side, we tested him with a variety of tasks involving the discrimination of motion in the same apparatus as was used for the static tests. In the first stage, we examined his discrimination of speed, direction, and two-dimensional shape generated by differences in speed and direction. Six of the tests involved first-order motion and the seventh involved second-order motion. These are described first. It was the difference in his performance when viewing first- and second-order motion that led us to compare them directly with a variety of tests that are described separately in Section C.

Experiment 1: Local speed discrimination

The task, described in detail by Vaina (1989) and Vaina et al. (1990*a*,*b*), measured the perception of relative speed of two simultaneously presented sparse random-dot kinematograms (density 2 dots/deg^2) displayed in two rectangular apertures, one above the other and each subtending 5 deg × 10 deg with 6 deg between their centers (Figs. 3A and 3B).

In the first speed discrimination task (shown schematically in panel A), each dot trajectory changed randomly from frame to frame, but the speed was the same for all the dots within an aperture. In the second speed discrimination test (panel B) within each aperture, all the dots moved in the same direction and at the same speed. In both speed tasks, the variable was the ratio of speed difference between the two apertures. The standard speed, present in one or other aperture at random, was 3 deg/s and the speed in

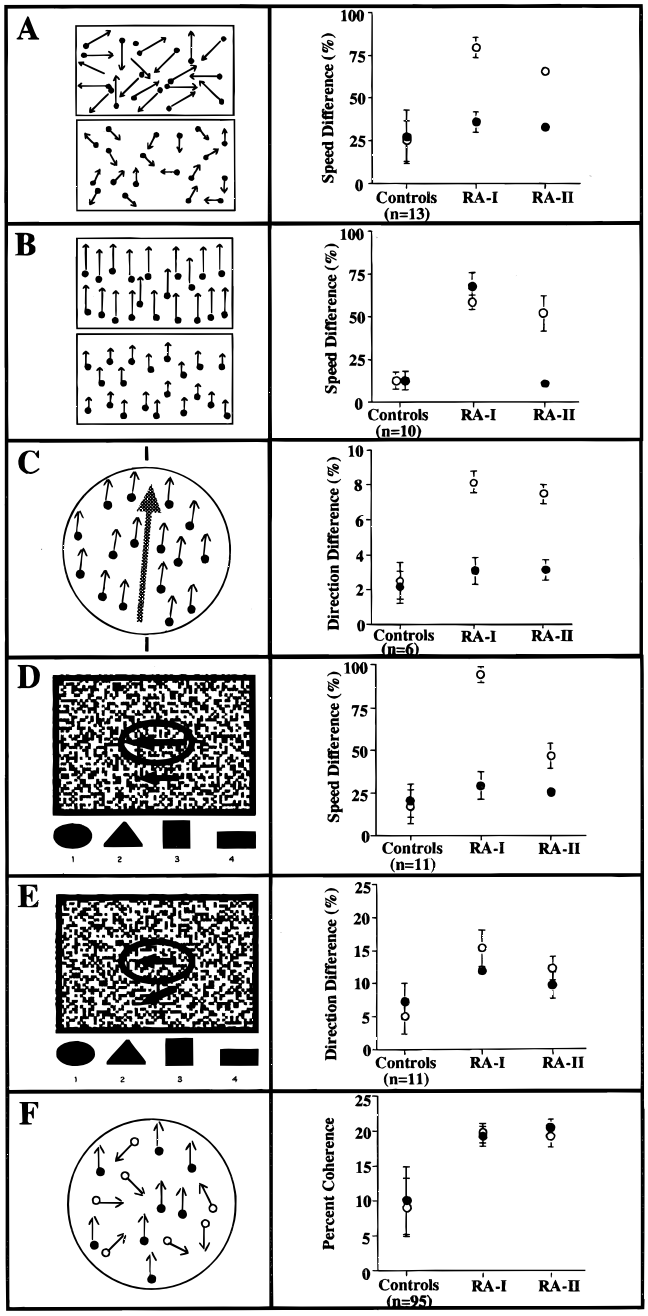

Fig. 3. On the left of each pair of boxes are schematic views of the initial set of displays used to test RA's motion vision. On the right are the results for each test. The number of control subjects varied from 6 to 95, according to the test. RA-I and RA-II refer to testing sessions that took place roughly 2 months and 20 months, respectively, after his stroke. Note that RA was selectively impaired in his left visual hemifield on all the motion tasks except the test of global motion, shown in F, where he was impaired in both hemifields.

the other aperture varied from trial to trial according to the adaptive staircase procedure, starting at 6 deg/s (ratio of 2). To prevent the consistent use of confounding cues (e.g. distance traversed by the dots in the constant direction stimulus—panel B), we randomly varied the standard speed stimulus duration by ± 20%. In a 2AFC procedure, subjects were asked to indicate the aperture in which the dots moved faster.

In the first speed discrimination task (panel A), the performance of 13 normal control subjects was compared to RA's and Fig. 3A shows that for stimuli presented in his left visual field he was, and remained, significantly impaired compared to the control subjects and his own performance in the right visual field. At threshold, the controls required a difference in speeds of about 25% to perform the discrimination, while RA's thresholds for stimulus presented in the left visual field were 80% (for RA-I) and 66% (RA-II). Both were more than 10 standard deviations above the scores of normal controls computed by a Z score. In his intact, right visual field he was within the normal range. Moreover, his impaired performance for stimuli presented in the left visual field was little altered 18 months after initial testing (RA-I and RA-II). Although RA's initial inferior left quadrantic field defect had disappeared by the time the performance noted as RA-II was recorded, it is possible that his deficit might be due to the fact that the dots in the lower aperture fell at least partially in this region of his left visual field. We therefore repeated the task with the entire stimulus array displayed in the upper left or right quadrant. The results from RA and two age-matched normal controls were essentially unaltered (there was no significant statistical difference in the subjects' performance on the two speed tasks).

A similar difference in performance between RA and 10 normal control subjects was found for the second speed discrimination task where the dots moved in the same direction but with different speeds (Fig. 3B). While the threshold for speed difference of the control subjects was roughly 13%, RA's initial threshold for stimuli presented in either visual field was almost 60%, which is 15 standard deviations above the scores of the normal controls computed by a Z score. However, his performance in the right visual field became normal (see RA-II), whereas his threshold in the left visual field remained high at 50%, that is 12 standard deviations from the threshold of the controls and his own in the right visual field.

Experiment 2: Direction discrimination

The stimulus consisted of a sparse random-dot kinematogram displayed in a circular aperture 10 deg in diameter. Dot density was 2 dots/deg^2 and speed was 3 deg/s. All the dots moved upwards and at a variable angle to the left or right of true vertical (Fig. 3C), indicated by a short and clearly visible line placed 0.5 deg above the display aperture. In a 2AFC procedure, subjects were asked to determine whether the dots moved obliquely to the right or the left with respect to the vertical line.

Fig. 3C shows the results from RA and six age-matched normal controls. While the control subjects and RA required roughly a 2-deg deviation from vertical in order to discriminate direction accurately in the right visual field, for stimuli presented in his left visual field RA required roughly 8 deg, which is 4 standard deviations above the scores of the normal controls computed by Z score. Again, his performance did not change significantly when the stimulus was entirely confined to the upper portion of his left visual field, above his initial field defect. The deficit remained stable for more than 18 months (RA-I and RA-II). His high threshold in the left hemifield contrasts strikingly with his normal threshold in the same hemifield for static stimuli in an otherwise similar task (Fig. 2D).

Experiment 3: Discriminating shape created by relative motion

Since RA was impaired on both speed and direction discrimination for stimuli presented in the visual field contralateral to his

lesion, but his ability to perceive static shape from a noisy masking background was normal, we investigated his ability to perceive two-dimensional shapes generated either by a difference in direction from the motion of the background or by a difference in speed. The display (Figs. 3D–3E) consisted of a dense field of random dots shown in a 10 deg × 24 deg aperture. One of four shapes (Figs. 3D–3E at the bottom) within an area subtending 2 × 2 deg^2 becomes visible when the dots within its boundary move in a different speed or direction from the moving dots in the background. At the beginning of a trial, a shape appears in the center of the display and moves horizontally in the same direction as the background but slower (Fig. 3D) or in a different direction (maximum 90 deg difference) from the background but with the same speed (Fig. 3E). The speed of the background is always 3 deg/s. After traversing 5 deg, the direction of motion of the figure and background reverse. The size of the dots was 4 arcmin.

The difference (direction or speed) between the shape and background was systematically varied using the adaptive staircase procedure and in a 4AFC procedure, where observers indicated which of the four figures displayed at the bottom of the screen matched the moving shape. In the speed condition the differences in speed were produced by varying the speed in logarithmic steps, 32 steps per decade, over a range of 3 decades, from 100 to 0.1%. In the case of a difference in direction between motion of the background and the stimulus dots, the variable represents the difference in direction of motion as a percentage of 90 deg.

Fig. 3D (right) shows the results of the discrimination of shape created by differences in speed. The 11 normal control observers required about 20% speed difference in order to reliably identify the shape. On the other hand, in his left visual field RA initially required almost 100% speed difference to identify the moving shape reliably, while in the right visual field his performance was not statistically significantly different from that of the controls. His performance in the left visual field improved substantially by the time that he had full recovery of the visual field, but still remained in the impaired range as compared with his own results in the right visual field and the results from the normal controls (his thresholds in both RA-I and RA-II were, respectively, 19 and 7 standard deviations above the scores of the controls computed by a Z score).

Fig. 3E (right) portrays the performance of RA and of the same 11 control subjects on the discrimination of the shape created by differences in direction of motion. Initially, his thresholds for stimuli presented in either visual field were elevated compared with those of the control subjects. Although his performance in the right visual field was subsequently no different from normal, he remained impaired on the left (thresholds were, respectively, 4.5 and 3.5 standard deviations above the scores of the controls).

Experiment 4: Motion coherence

This task is described in detail in Vaina and Cowey (1996). The stimuli (Fig. 3F, left) were stochastic random-dot cinematograms with a coherent motion direction signal of variable strength embedded in a masking motion noise, presented in a circular aperture 10 deg in diameter and with dot density of 2 dot/deg^2 and speed of 3 deg/s. The algorithm by which the micropatterns were generated, adapted from Newsome and Paré (1986), is described in detail in Vaina et al. (1990*a*). Briefly, during each trial some given proportion of dots moved in identical manner from frame to frame creating the impression of global motion. Especially at lower correlation probabilities, it was unlikely that the perceiver could follow a single dot or even a local cluster of dots over several frames in order to perceive a single direction of motion. Thus, the impression of movement could only be derived from a global computation, which integrated local motion measurements.

Fig. 3F (right) shows data from 95 control subjects and RA. The patient was conspicuously impaired on this task in *both* visual fields, and his performance remained unchanged even after his left visual-field defect had recovered. To perceive reliably the global direction of motion in the display, he needed twice as many correlated signal dots as the normal controls. This task was given to RA on every visit to the laboratory, and his performance remained consistently the same; his thresholds in both visual fields were roughly 4 standard deviations above the mean score of the normal controls.

Experiment 5: Discrimination of the direction of second-order motion: Flickering bar

Discrimination of direction in second-order motion was measured using a stimulus adapted from Albright (1992) and shown schematically in Fig. 4. The display, 10 × 10 deg^2, consisted of a static dot pattern (50% white, 50% black) over which was displaced an imaginary square-wave grating of spatial frequency 0.2 cycle/deg and temporal frequency 6 Hz, or 0.5 cycle/deg and 2 Hz, resulting in a speed of 30 deg/s and 4 deg/s, respectively. Mean luminance across the entire display was constant. The square wave was composed of flickering dots, created by inverting the contrast of a given percentage of dots in each frame within the bounds of each square wave. The percentage of the dots that flicker was varied by the adaptive staircase procedure (three consecutive correct responses: 1 step down; any error: 1 step up) and determined the "contrast" of the moving bar. Subjects had to indicate the direction of motion, up, or down. The stimulus was present for 0.5 s on each trial.

Fig. 4 shows the percentage of flickering dots needed to discriminate with 84% accuracy between opposite directions of motion of the travelling square-wave pattern. The 18 controls and RA had very similar results for stimuli presented in either visual field. This was initially surprising, given RA's clear impairment on some of the preceding motion tests. However, the *flickering bar* test is an example of second-order motion whereas the others involved first-order motion (for a detailed discussion and stimulus analysis see Clifford and Vaina, submitted). As second-order motion can be selectively disturbed by cortical damage (see Introduction), we used further tests of the two types of motion to see whether a cortical lesion can also impair first-order motion while leaving second-order motion intact.

C: Comparison of first- and second-order motion

Experiment 6: D-max for first-order and second-order Gabor micropatterns

The procedure was adapted from that described by Boulton and Baker (1993). Using a 2AFC procedure and a method of constant stimuli, observers had to indicate the apparent direction of displacement (left or right) between two successive displays, each lasting 105 ms, of an array of micropatterns (see Fig. 5). In between trials the display was of mean luminance, L_0. Each micropattern was a Gabor function, i.e. an oriented unidimensional sine-wave grating multiplied by a two-dimensional Gaussian window. The micropatterns were defined by:

$$L(x,y) = L_0\{1 + C\exp[-(x^2/2\sigma_x^2 + y^2/2\sigma_y^2)]$$

$$\times \cos(2\pi x/\lambda + \psi)\}$$

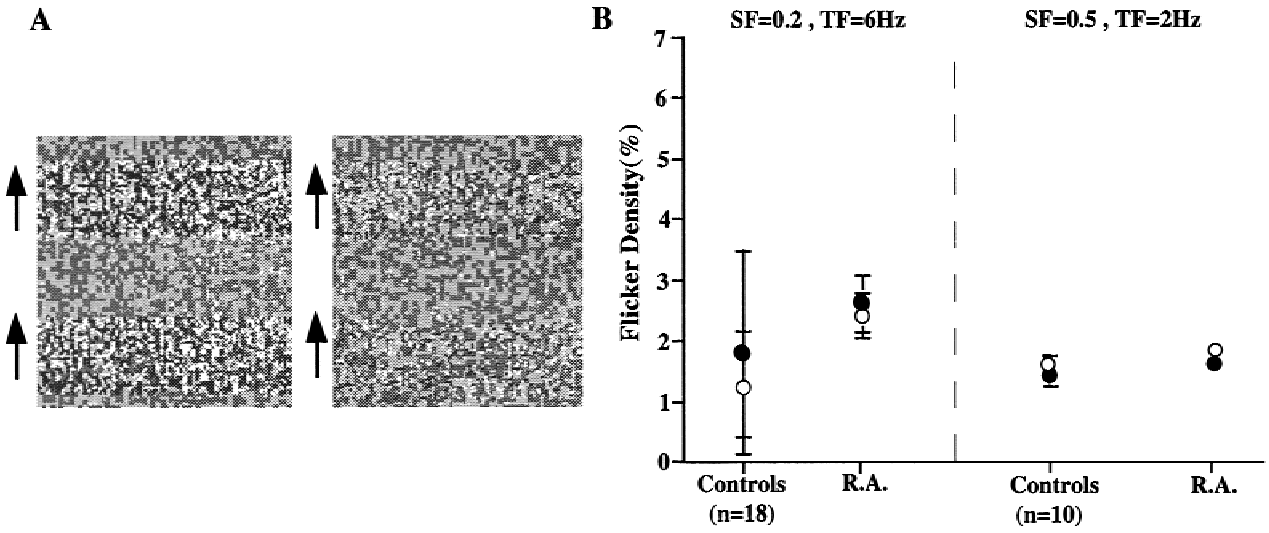

Fig. 4. The two displays on the left each show a single frame of the arrangement used to produce a flickering and apparently moving bar in Experiment 5. The illustrated flicker density is 50% and 20%. The minimum flicker density for 80% correct discrimination of the direction of apparent movement of a bar at two different spatial and flicker frequencies is shown at the right. Patient RA was not impaired in either visual hemifield when compared with control subjects.

where L_0 is the mean luminance, C is contrast, σ_x is the horizontal Gaussian width parameter, σ_y is the vertical Gaussian width parameter, λ is the wavelength of the cosine wave component, and ψ is phase of the cosine wave.

The values used were $C = 25\%$, $\psi = 0$, $\lambda = 16$ pixels $= 2.25$ cycles/deg and $\sigma_x = \sigma_y = (0.75/\sqrt{2})\lambda$ so that the envelope of the micropatterns was circular, $L_0 = 6.2$ cd/m^2. The micropatterns were grouped in two strips across the top and bottom of the display, each strip subtending 3 deg high $\times$ 11.5 deg wide, and separated by 2.5 deg at a viewing distance of 150 cm. There was no interstimulus interval. On each trial, the micropatterns were placed on a notional grid and to prevent periodicity and clustering effects the position of each micropattern was randomly jittered by 1/3 of the grid spacing about the grid location. Values of positional jitter were independently selected each trial for each micropattern. Wrap-around was employed at the display boundaries.

Observers maintained gaze on a fixation mark placed at midline level 0.5 deg to the left or right margin of the display, and initiated each trial *via* a button press. A method of constant stimuli was used and performance was measured for a range of displacements from 0.25λ to 3λ, in increments of 0.25λ. For each experimental run, eight displacements were chosen and presented in pseudorandom order 20 times each. The run was repeated five times.

There were two stimulus conditions differing only in the number of micropatterns presented. In the first-order motion condition, 66 micropatterns were shown on a notional grid of 11 columns and three rows in each strip (Fig. 5A, top). In the second-order motion condition, there were 36 micropatterns shown on a notional grid of six columns and three rows in each strip (Fig. 5B, top). In a series of psychophysical studies of this stimulus, Boulton and Baker (1991, 1993) have shown that performance on direction discrimination in the dense, but not in the sparse, pattern is proportional to the direction information in the spatiotemporal Fourier power spectrum of the stimulus. This qualifies the dense pattern as first-order motion involving early linear filtering. The difference in performance between the high and low density patterns suggests that in the latter the spatial-frequency information is not used by the visual system. One way to ignore this information but preserve knowledge of the position of the stimulus elements is by applying a nonlinear operation, such as full-wave rectification of the signal after the initial first-order filter. It has been shown that this results in a signal that can then be analyzed by conventional, first-order motion detectors (Chubb & Sperling, 1988). In summary, Boulton and Baker's results and the data shown below from the normal control presented here could be accounted for by models for second-order motion mechanisms.

The results for direction discrimination from RA and a matched control subject are shown as percentage errors as a function of the displacement of the stimulus for 66 micropatterns (Fig. 5A, bottom) and 36 micropatterns (Fig. 5B, bottom), respectively. Displacement is shown as multiples of the wavelength of the cosine component of the Gabor-micropattern varying from 0.25 cycle to 3 cycles in steps of 0.25 cycle. The first part of Fig. 5A (bottom) (up to 1.5 cycles/deg) is characteristic of RA's preference for using second-order motion. Whereas the results of the normal control observer indicate that he looks at the carrier, which is luminance based, RA's performance indicates that he uses the motion of the envelope component, which is second-order. As discussed by Boulton and Baker (1993) the second-order or nonlinear mechanism detects the motion of the contrast envelope of the stimulus without making use of the internal structure of the envelope. For the second-order motion (Fig. 5B, bottom), the pattern of his responses is very similar, although noisier, to that of the normal control. (Further 23 young normal controls (ages 19–24) have since been tested with both experiments and their mean results fall within $\pm$ 1 S.D. of the mean results obtained by the normal control age-matched to RA and reported here.)

In an additional experiment (kindly suggested by C.L. Baker) that addresses the second-order motion, we changed the orientation of the cosine component between the two frames. If the nonlinear mechanism does not make use of the information within the micropattern, the orientation change should have no effect. The results of RA and 15 (young) normal controls were essentially identical

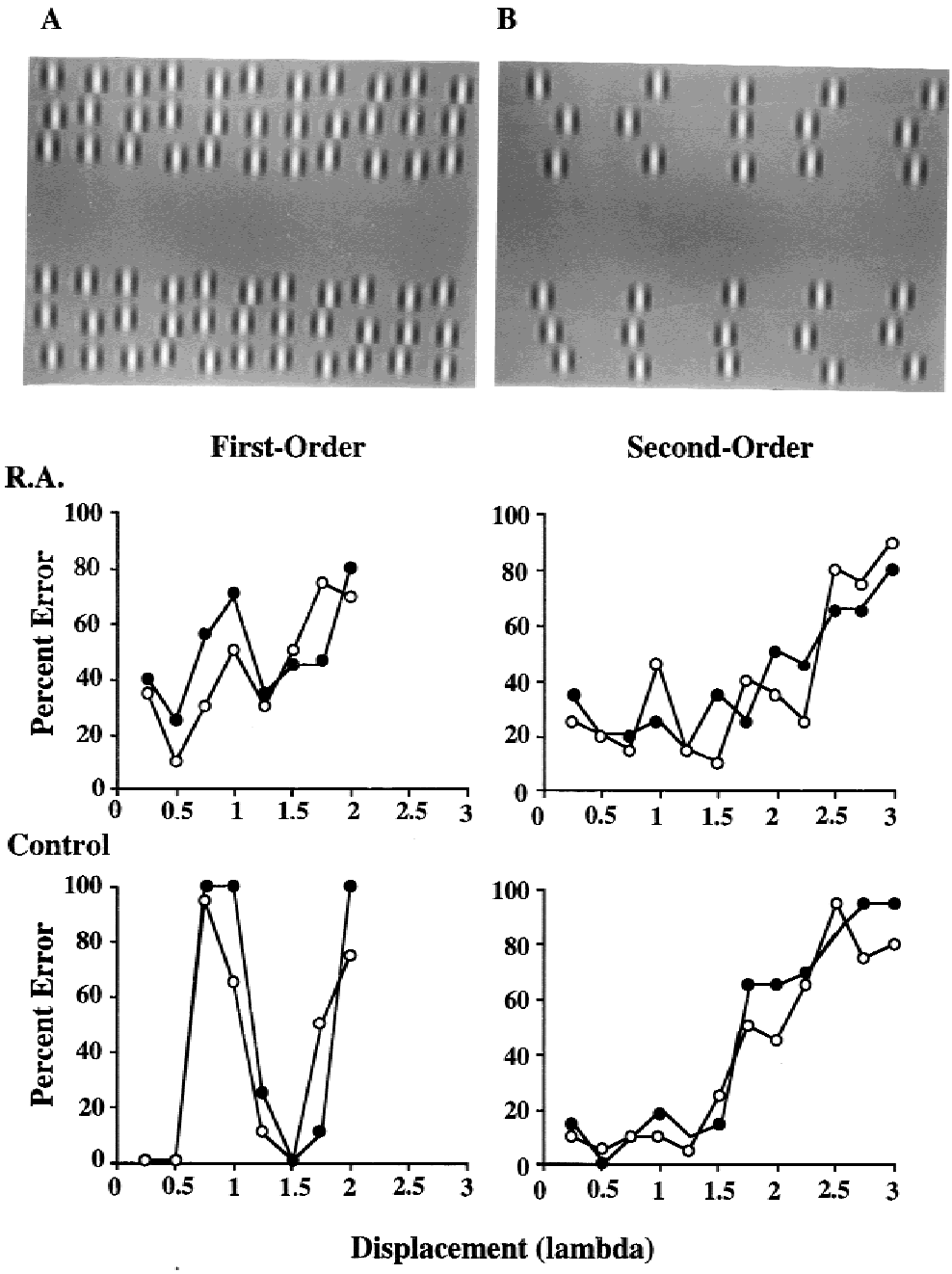

Fig. 5. The results of testing thresholds for discriminating left/right displacement of pseudorandomly distributed micropatterns (Gabor patches). In second-order motion, there was no difference between the performance of RA and a matched control subject with respect to second-order motion in either visual hemifield. However, with first-order motion, the control subject shows the characteristic error function with respect to the multiple of the wavelength of the cosine component of the Gabor micropattern whereas RA continued to perform as if he was responding only to the second-order envelope of the motion stimulus.

to those in Fig. 5B, showing that RA was indeed using the non-linear mechanism underlying second-order motion.

Experiment 7: D-max, using first-order and second-order dense random-dot patterns

In this test, we measured direction discrimination performance for two varieties of briefly presented two-frame dense random dot kinematograms (Fig. 6). The stimulus field subtended 10 × 10 deg arc, and was presented against a uniform gray background (9.5 cd/m^2). The stimulus area was divided into a notional grid of 38 × 38 blocks, each subtending 16 arcmin × 16 arcmin.

Each block is a dense random-dot microtexture consisting of pixels whose luminance is one of 256 possible gray levels. The dots defining the microtexture can have one of two states: on or off, represented by different gray levels. The number of "on" and "off" dots within a block is evenly distributed. The mean lumi-

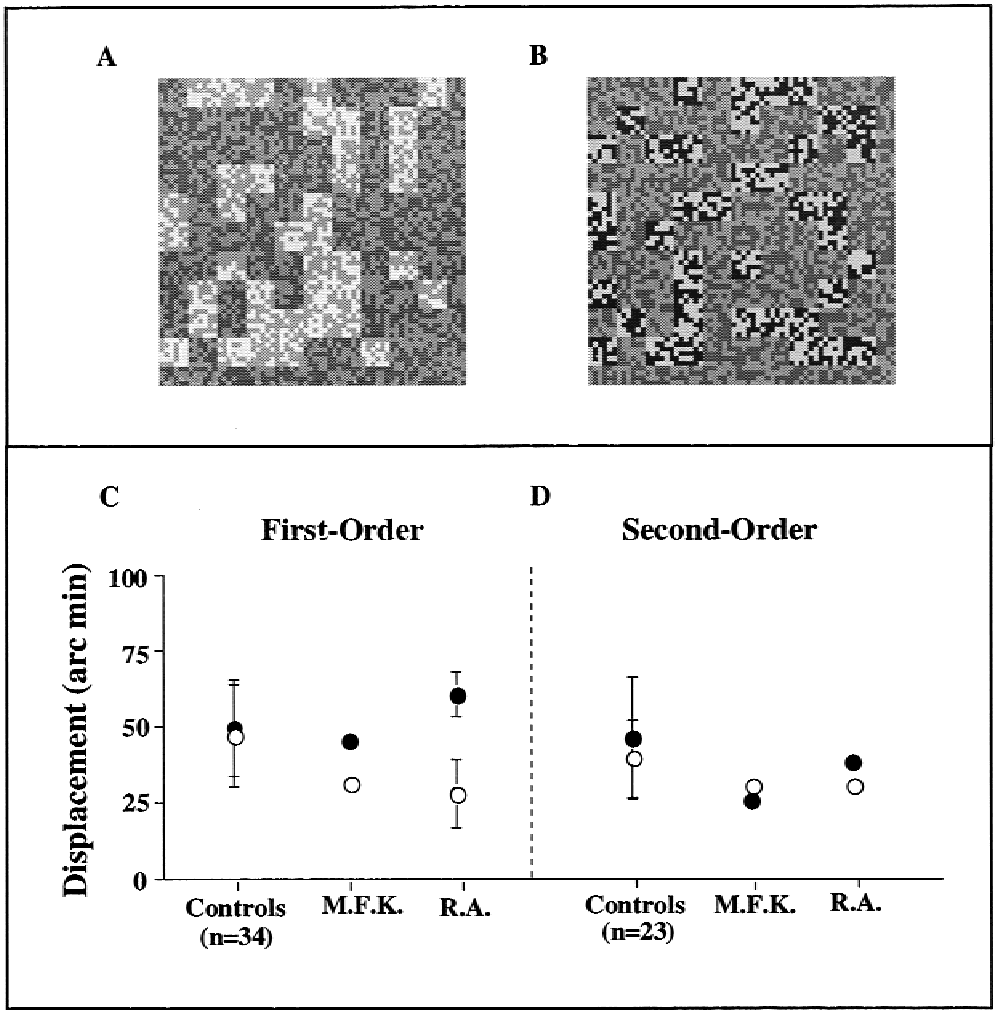

Fig. 6. A and B show single frames of the displays used to measure direction discrimination in random-dot kinematograms. In A, the motion is first-order: a group of micropatterns differing from the background in luminance is shifted left or right. In B, the motion is second-order: the shifting micropatterns differ from the background in contrast but not mean luminance. C and D show the performance of RA and control subjects on the two tasks. RA was impaired in his left visual hemifield on the first-order but not on the second-order task.

nance of a block is the average of its "on" and "off" dots. Its contrast is the ratio of the difference in luminance of "on" and "off" dots divided by twice the mean luminance. A block can differ from the background either in mean luminance but not contrast (first-order motion), or in contrast but not mean luminance (second-order motion), and in both cases is called a token. Whether a block is token or background, it is randomly assigned at the beginning of every trial and token-block density remains constant at 42% throughout the test. The "on" and "off" state of the dots in the background and tokens is reassigned at random, creating flicker. The mean luminance of first-order motion token blocks was 12.3 cd/m^2 and contrast within the block was 0.2, while the mean luminance of second-order blocks was 9.5 cd/m^2 and mean contrast was 0.6. The mean luminance of the background was in both cases 9.5 cd/m^2 with mean contrast of 0.2.

Motion stimuli consisted of two successively presented frames (frame duration 45 ms, and zero interframe interval). From one frame to the next, the token blocks are shifted coherently either to the left or to the right, with the remaining background acting as a viewing window. The specific spatial pattern of texture defining the tokens and the background is varied from frame to frame by randomly changing the component pixels (from "on" to "off" and *vice versa*), yet keeping their mean luminance and contrast identical throughout the trial.

Subjects were instructed to keep their gaze on a fixation mark 2 deg to the left or right of the lateral edge of the display. Using 2AFC they reported whether the direction of motion was to the left or right. Stimuli were varied by the adaptive staircase procedure and threshold for the maximum displacement for which observers correctly perceived the direction of motion was averaged over the last six reversals.

Fig. 6A, bottom left, shows the results for RA and 34 normal controls varying in ages, and a control subject (subject MFK) exactly age- and education-matched to RA. The *y* axis indicates the threshold of displacement (D-max), in arcmin, for which RA and the controls could reliably perceive left or rightward motion. The D-max values on the first-order task of the normal controls were similar to those previously reported (Vaina et al., 1994). RA's D-max is smaller in the left visual field (2 standard deviations lower than in the right visual field, as computed with

Z scores, $P < 0.05$). However, as shown in Fig. 6B, bottom, the D-max values for second-order motion were very similar in all subjects and there was no statistical difference between hemifields.

Experiment 8: Direction discrimination in first-order and second-order global motion

The previous experiments addressed local motion measurements which, at least for the first-order displays, are presumably mediated by motion mechanisms that are spatially local. To determine whether the dissociation between RA's ability to process direction in first- and second-order motion stimuli is also present for spatially global stimuli, where purely local computations are inadequate, we used a pair of first- and second-order global motion tests in which to extract direction effectively the subject must integrate motion information over the entire stimulus. RA also performed another global motion task (Experiment 4; Fig. 3F) on which his performance was consistently in the range of mild impairment.

The displays in these tasks are like those described in Experiment 7, except that the strength of the motion signal in the stimulus was varied by changing the proportion of the token-block micropatterns in a given trial that carry the same unidirectional motion signal. The remainder of the token-block micropatterns appeared from frame to frame at random locations, creating the impression of random textured flicker. When all the micropatterns reappear with the same spatial and temporal offset, the display appears as a cluster of micropatterns all moving to the left or to the right across the flickering background. The display was presented in a square aperture 10 deg in diameter, 2 deg left or right of a small dark gray fixation mark placed at eye level. The surround of the display was uniform gray (9.5 cd/m^2). Token density was 2 tokens/deg^2 and speed was 3 deg/s. The mean luminance of first-order micropatterns was 12.3 cd/m^2 and contrast was 0.2, while the mean luminance of second-order micropatterns was 9.5 cd/m^2 and contrast 0.6 (Fig. 7, top). Using the adaptive staircase procedure the stimulus was presented for 12 frames, each frame shown for 45 ms, with zero interframe interval. Observers were asked whether the global motion was rightward or leftward. Threshold proportion of signal tokens (percent coherent motion) necessary for reliable discrimination of stimulus direction was computed as the mean of the last six reversals in the staircase.

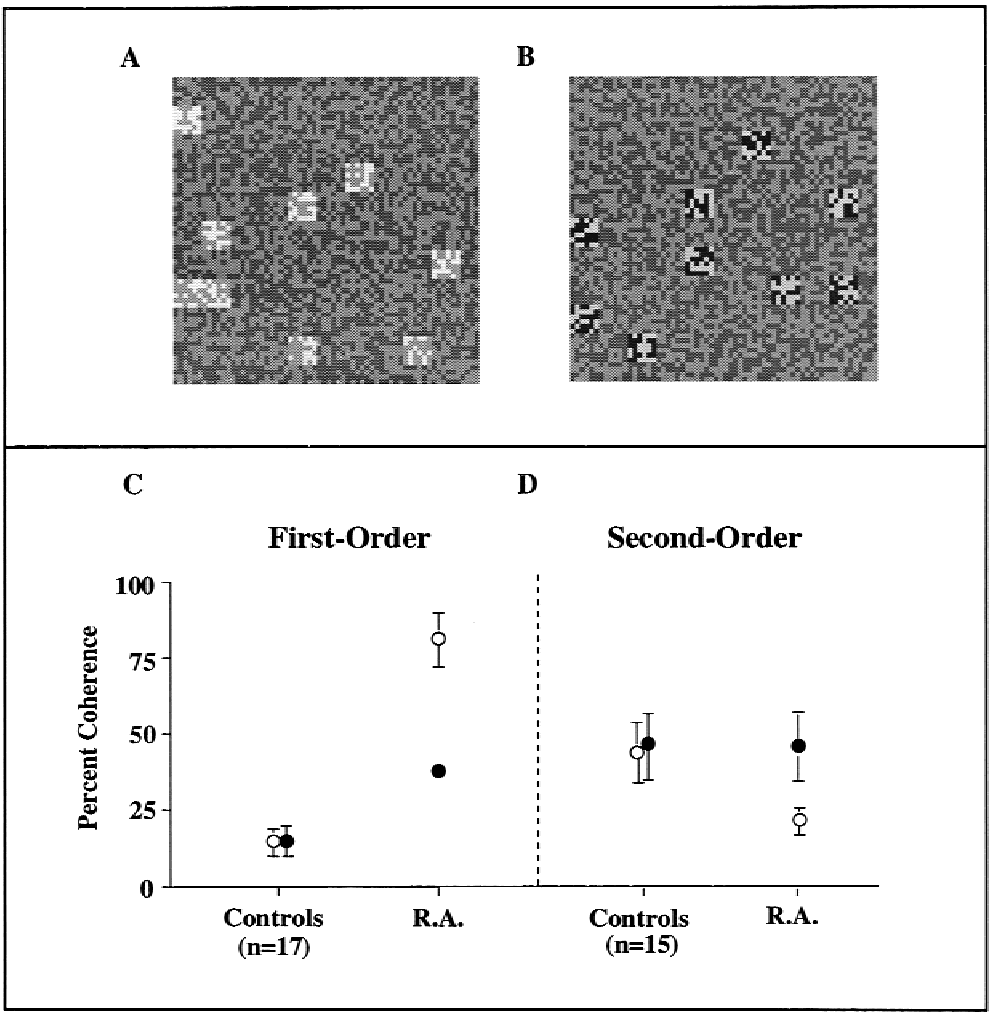

Fig. 7. At the top is shown a single frame of the display used to produce first-order (left) and second-order (right) global motion. The percentage coherence needed for 80% correct discrimination of direction, left or right, is shown below. RA was substantially impaired on first-order motion in his left hemifield but not impaired with second-order motion.

Fig. 7 (bottom left) shows data from RA and 17 normal control subjects on the first-order global motion task. RA's threshold coherence for 80% correct in each visual field was higher than that of the control subjects but dramatically so in his left visual field. Just as impressive is that compared with 15 normal controls, his threshold in both left and right visual fields was normal in the second-order global motion tasks. Thus, RA's elevated threshold in the left visual field on the first-order task cannot be explained merely by a greater sensitivity to flickering "noise" (in both background and stimulus) than in the control population or in his left visual field. It is possible that the much larger difference between his left and right hemifields on the first-order global motion test, shown in Fig. 7, and the global motion task of Fig. 3F bottom-left is that the former is low luminance and that the display contains a larger proportion of noise (combined from the "noise" token micropatterns and the flickering background). In his "impaired" hemifield RA was actually more than just marginally better at discriminating second-order motion than in his normal hemifield and in each hemifield of control subjects. Whether this reflects the helpful effect of reducing noisy signals from the damaged first-order system is unclear.

Experiment 9: Long-range motion

Braddick's original dichotomy of motion processes into short range and long range was based on spatial displacements over which motion can be detected. Second-order motion has been shown to depend on the spatial-frequency content of the stimulus (Boulton & Baker, 1993; Werkhoven et al., 1993) and we have seen in Experiment 8 that one of its main distinguishing characteristics is that it operates over much larger spatial displacements than first-order motion. These attributes have been also used to characterize the long-range motion process (Braddick, 1974) which is very similar to the second-order motion.

Here we use a long-range motion task, adapted from Green (1986), which is very similar to the low-density version of the stimulus in Experiment 8. The display consisted of two pairs of vertically oriented Gabor patches arranged at the four corners of an imaginary square centered on a cross-hair fixation mark (Fig. 8). The stimulus consisted of four consecutive frames, displayed twice in succession to give a total of eight frames in one trial. Fig. 8A shows a cartoon of each of the four frames. The viewer discerns movement from the change in position of the carrier frequencies. The Gabors of each pair have the same spatial frequency and during a "rotation" only the position of the Gabors changes, not their orientation. One pair of Gabors, the reference, was held constant at 5 cycles/deg. The other pair could have one of five different central spatial frequencies: 1, 1.7, 3, 5 and 10 cycles/deg. The separation between centers of like Gabors was 3.6 deg and for a 45 deg rotation each Gabor travelled 1.4 deg. The eight frames, each visible for 75 ms, interleaved with seven 45-ms stimulus intervals, were displayed in one of two sequences, corresponding to clockwise (presenting the frames in the order 1,2,3,4) or counterclockwise rotation (order 1,4,3,2). At 100% contrast each Gabor subtends 1.7 deg. Since Gaussian modulation effectively hides the edges of an object, the observed size of a *Gabor* is a function of the contrast of the *Gabor* and the contrast sensitivity of the subject. In all stimuli used, the contrast was above threshold.

Viewing distance was 125 cm and stimuli were displayed by the method of constant stimuli (24 trials per data point). Subjects were asked to maintain fixation on the cross hair and a 2AFC procedure was used to elicit responses of whether the Gabor patches appear to "rotate" in a clockwise or anticlockwise direction. Note that to solve this task *both* hemifields are needed, hence central fixation is appropriate.

To control for the possibility that subjects could use apparent contrast to identify corresponding Gabors, observers were shown all five Gabors and asked to adjust the contrast of each Gabor, using the mouse, until they all had the same apparent contrast. The contrasts were adjusted in the range of 100% to 50% contrast, in steps of 5%. Once the subject was satisfied that all Gabors had the same apparent contrast, the adjusted contrasts for each Gabor were recorded and used throughout the rest of the test for creating displays.

To be certain that the subjects perceived the whole stimulus, we devised a simple static control test. Four Gabor patches covering

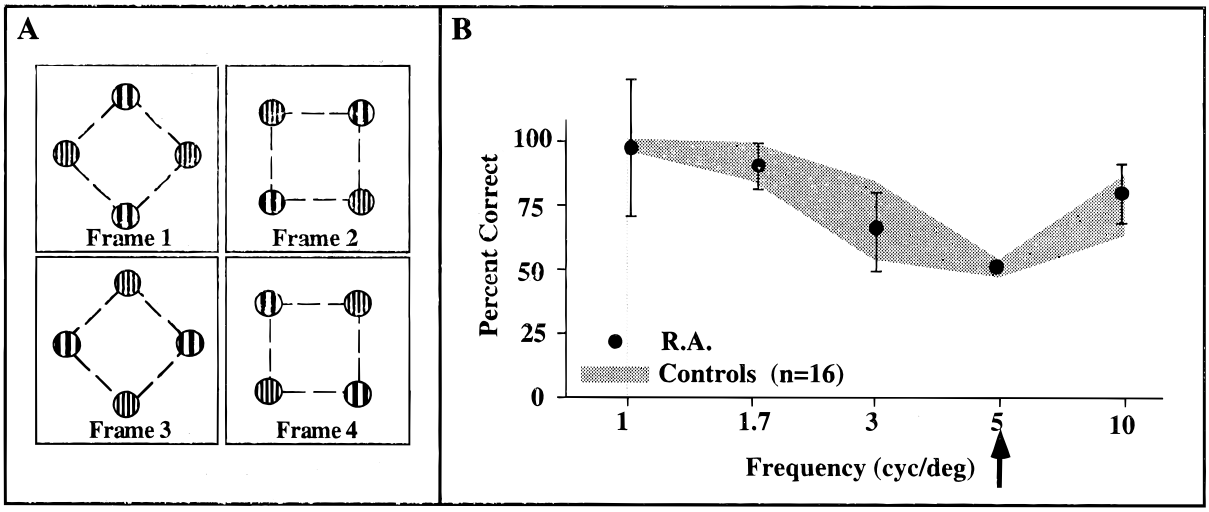

Fig. 8. On the left is shown the schema for generating second-order long-range motion using Gabor patches. One pair of Gabor patches was always 5 cycles/deg. On the right is shown percentage correct performance in judging the direction of apparent rotation, as a function of the spatial frequency of the other pair of patches. RA performed as well as the 16 normal control subjects.

the same spatial frequencies as in the *long-range motion* test were presented in the same configuration as shown in the left-most schematic display in Fig. 8A. The only difference was that the Gabor patches remained static. One patch, placed randomly in one of the four positions, differed in spatial frequency from the other three by the same ratios as in the motion task. The subject was asked to fixate the central cross mark and to pick out the odd Gabor patch. There were 20 trials in this task. RA's performance was also normal on the static control task.

The results on the Long-range motion test from RA and 16 control subjects are shown in Fig. 8. RA's performance was normal across the whole range of spatial frequencies.

Discussion

Our results show that throughout the two-year period during which we tested him after his stroke, RA was selectively impaired on various discriminations involving first-order motion. With the exception of depth perception based on binocular disparity, which remains impaired, and his identification of silhouettes displayed in noncanonical views, RA's performance on static stimuli was normal. The poor performance on the recognition of objects' silhouettes could indicate a mild object agnosia because it was not based on any inability to see the outline of the shapes. Although RA initially had a lower quadrantic field defect contralateral to his unilateral lesion, this could not explain either the presence or the selectivity of the disturbance of first-order motion perception because he was impaired even when the displays were confined to the upper quadrants and long after the quadrantic field defect had disappeared. In the first few weeks after his stroke, RA noticed that movement in his left visual field was not normal but this recovered swiftly and he is now unaware that his perception of some aspects of motion perception are impoverished. In this repect he is quite unlike a "motion blind" patient (see below). By analogy, he is more like someone with anomalous color vision, whether inherited or acquired, who finds nothing unusual about his vision and whose disorder is only apparent with special tests. RA's results raise several points for discussion.

How specific is the impairment?

In every motion test on which RA was impaired, first-order motion was the principal or only cue. In every test in which second-order motion exclusively or predominantly provided the cues, he was not impaired. The results also indicate that the dissociation was not simply between local and global perception of motion, because it was the latter that had to be judged in the first-order *and* second-order displays of Experiment 8. What remains unclear, and was not specifically addressed in these experiments, is whether the defect is confined to the discrimination of speed and direction of first-order unidirectional global motion or whether it also embraces more complex forms of motion, such as rotational, or centrifugal and centripetal (providing the appearance of receding and looming respectively), heading discrimination and perception of three-dimensional structure from motion. Recently, we addressed RA's ability to perceive these types of complex motion (Vaina et al., 1996*b*) and found that his performance was normal in all except on the discrimination of some forms of three-dimensional structure from motion and heading with a curved path. These latter tasks might rely on a more accurate computation of speed or direction than RA's, or possibly different stimulus displays differentially recruit first- or second-order motion.

The significance of the impairment

The Introduction discussed various theories of how motion might be computed and represented in the cerebral cortex. The results of RA's performance on a wide variety of first- and second-order motion stimuli indicate that second-order motion, on which his performance was normal, cannot be solely generated from the mechanisms in visual cortex that provide the basis for the perceptual awareness of first-order motion. Of course it could be generated from first-order signals in cells and areas that are not involved in or are insufficient for normal perceptual awareness of first-order motion. But the principal outcome is that RA provides evidence that the processing of first- and second-order motion at the cortical level is at least partially segregated and that the segregation is grossly regional as well as functional. His defect is complementary to that of patient FD (Vaina & Cowey, 1996), who is impaired on second- but not first-order motion, and taken together the two patients indicate that second-order motion is not simply generated from first-order mechanisms operating at an earlier stage of a hierarchy. Whether the two mechanisms are related to parvocellular and magnocellular pathways, respectively, as proposed by Boulton and Baker (1993), is not addressed in the present study. Like patient FD, RA has a defect that arises from a cortical lesion involving only a small part of extrastriate visual cortex. A much larger lesion can produce the condition of akinetopsia (see Zeki, 1991, for review), in which the disturbance of motion perception is more extensive, more evident to the patient, and disabling. Presumably this indicates that areas other than those damaged in FD and RA are involved, as might be expected from the extensive physiological specialization that has been reported for various "movement areas" in extrastriate cortex of macaque monkeys (Dupont et al., 1994; Orban et al., 1995; Vaina, 1996). However, even in akinetopsia the perception of some forms of motion can be spared, e.g. structure from motion and biological motion (Vaina et al., 1990*a*) suggesting that the regional specialization is even more extensive than hitherto suspected, and certainly not confined to first- and second-order.

Where is the effective lesion in RA?

The cortical damage in RA is chiefly superior to the calcarine fissure, in the medial third of the occipital cortex. According to functional neuroimaging maps (Tootell et al., 1995), it almost certainly involves parts of areas V2 and V3, and perhaps adjacent areas. It is remote from human area MT/V5. However, there is at present no ready means of knowing whether it involves fibers from V1, which in macaque monkeys provide a direct input to area MT and which provide an important component of the input that creates the directional sensitivity of many of its cells (Rodman & Albright, 1989). It is therefore possible that RA's impaired motion perception reflects the role of MT in first-order motion processing. We are preparing to examine this question in functional neuroimaging investigations of RA, including the localization of cortical potentials evoked by first-order displays, and in experiments on macaque monkeys trained to discriminate the direction and speed of motion with the same displays used to test RA.

Bilateral effects

RA's lesion is unilateral but he was mildly impaired in his ipsilateral hemifield for some types of first-order motion, for example, the motion coherence of Experiment 4. We have no convincing explanation for this but it was not caused by any failure on his part

to fixate the center of the display rather than eccentrically on these particular tasks. As described in the Methods, his fixation was monitored and it was easy to distinguish left and right eccentric fixation from straight-ahead viewing. One possibility is that the lesion mildly impairs motion processing in visual areas in the intact hemisphere by damaging the input it normally receives from the other hemisphere. Even though a stimulus is confined to one hemifield, its processing in the contralateral hemisphere might not be normal when the input from the other hemisphere is disrupted or processing involves neurons with receptive fields that cross the vertical meridian (Gattass et al., 1981, 1988). Visual areas 2 and 3 in the human brain, where RA's lesion lies, are extensively connected with their counterparts in the opposite hemisphere (Clarke & Miklossy, 1990). As in monkeys, the interhemisphere connections are limited to the cortex representing a strip of retina straddling the vertical meridian and wide enough to include the displays presented to RA, or at least parts of them (Horton & Hoyt, 1991). Removing this input might alter the receptive-field properties of cells in the undamaged hemisphere, both immediately, and following functional reorganization (Kaas et al., 1990).

Acknowledgments

This work was supported in part by the NIH Grant EY07861 to L.M.V., by an Oxford McDonnell-Pew Network Grant to A.C. and L.M.V., and by MRC Grant G971/397/B to A.C. We are indebted to Curtis Baker and George Sperling for carefully reading the manuscript and making excellent and extensive suggestions. We also thank Jose Diaz for programming the psychophysical stimuli and Jane Boulton for fruitful discussions about the Boulton and Baker experiment, and Charles Chubb for discussing preliminary versions of Experiment 8.

References

Albright, T.D. (1992). Form-cue invariant motion processing in primate visual cortex. *Science* **255**, 1141–1143.

Baker, C.L., Hess, R.F. & Zihl, J. (1991). Residual motion perception in a motion-blind patient, assessed with limited-lifetime random dot stimuli. *Journal of Neuroscience* **11**, 454–461.

Barbur, J.L., Watson, J.D., Frackowiak, R.S.J. & Zeki, S. (1993). Conscious visual perception without V1. *Brain* **116**, 1293–1302.

Boulton, J.B. & Baker, C.L. (1991). Motion detection is dependent on spatial frequency not size. *Vision Research* **31**, 77–87.

Boulton, J.C. & Baker, C.L. (1993). Different parameters control motion perception above and below a critical density. *Vision Research* **33**, 1803–1811.

Braddick, O. (1974). A short-range process in apparent motion. *Vision Research* **14**, 519–527.

Cavanagh, P. & Mather, G. (1989). Motion: The long and short of it. *Spatial Vision* **4**, 103–129.

Chubb, C. & Sperling, G. (1988). Drift-balanced random stimuli: A general basis for studying non-Fourier motion perception. *Journal Optical Society of America A* **5**, 1986–2007.

Chubb, C. & Sperling, G. (1989). Two motion perception mechanisms revealed through distance-driven reversal of apparent motion. *Proceedings of the National Academy of Sciences of the U.S.A.* **86**, 2985–2989.

Clarke, S. & Miklossy, J. (1990). Occipital cortex in man: Organization of callosal connections, related myelo-and cytoarchitecture, and putative boundaries of functional visual areas. *Journal of Comparative Neurology* **298**, 188–214.

Derrington, A.M. & Badcock, D.R. (1985). Separate detectors for simple and complex grating patterns? *Vision Research* **25**, 1869–1878.

Derrington, A.M., Badcock, D.R. & Henning, G.B. (1993). Discriminating the direction of second-order motion at short stimulus durations. *Vision Research* **33**, 1785–1794.

Dupont, P., Orban, G.A., De Bruyn, B., Verbruggen, A. & Mortelmans, L. (1994). Many areas in the human brain respond to visual motion. *Journal of Neurophysiology* **72**, 1420–1424.

Efron, R. (1968). What is perception? In *Boston Studies in the Philosophy of Science, Vol. IV*, ed. Cohen, R., pp. 137–173. New York: Humanities Press.

Farnsworth, D. (1943). The Farnsworth-Munsell 100-hue and dichotomous task for color vision. *Journal Ophthalmological Society of America* **33**, 568–578.

Gattass, R., Gross, C.G. & Sandell, J.H. (1981). Visual topography of V2 in the macaque. *Journal of Neurophysiology* **46,** 621–638.

Gattass, R., Sousa, A.P.B. & Gross, C.G. (1988). Visuotopic organization and extent of V3 and V4 of the macaque, *Journal of Neuroscience* **8**, 1831–1945.

Georgeson, M.A. & Harris, M.G. (1990). The temporal range of motion sensing and motion perception. *Vision Research* **30**, 615–619.

Green, M. (1986). What determines correspondence strength in apparent motion? *Vision Research* **26**, 599–607.

Grzywacz, N.M., Watamaniuk, N.J. & McKee, S.P. (1995). Temporal coherence theory for the detection and measurement of visual motion. *Vision Research* **35**, 3183–3203.

Hess, R.F., Baker, C.L. & Zihl, J. (1989). The "Motion-Blind" patient: Low-level spatial and temporal filters. *Journal of Neuroscience* **9**, 1628–1640.

Holliday, I. & Anderson, S.J. (1994). Different processes underlis the detection of second-order motion at low and high temporal frequencies. *Proceedings of the Royal Society* (London) **257**, 165–173.

Horton, J.C. & Hoyt, W.F. (1991). Quadrantic visual field defects. *Brain* **114**, 1703–1718.

Ichikawa, H., Hukami, K. & Tanabe, S. (1983). *Standard pseudoisochromatic plates–Part 2 (for acquired color vision defects)*. Tokyo-NY: Igaku-Shon.

Johnston, A., McOwan, P.W. & Buxton, H. (1992). A computational model of the analysis of some first-order and second-order motion patterns by simple and complex cells. *Proceedings of the Royal Society B* (London) **250**, 297–306.

Kaas, J.H., Krubitzer, L.A., Chino, Y.M., Langston, A.L., Polley, E.H. & Blair, N. (1990). Reorganization of retinotopic cortical maps in adult mammals after lesions of the retina. *Science* **248**, 229–231.

Kennedy, D.N., Filipek, P.A. & Caviness, V.S. (1987). Semi-automated image segmentation in multi-slice magnetic resonance images. *Proceedings of the Society of Magnetic Resonance Medicine* **6**, 378.

Kennedy, D.N., Filipek, P.A. & Caviness, V.S. (1989). Automated segmentation and volumetric calculation in cross sectional magnetic-resonance imaging. *IEEE Transactions on Medical Imaging* **8**, 1–7.

Ledgeway, T. & Smith, A.T. (1994). Evidence for separate motion-detecting mechanisms for first- and second-order motion in human vision. *Vision Research* **34**, 2727–2740.

Marr, D. & Ullman, S. (1981). Directional selectivity and its use in early visual processing. *Proceedings of the Royal Society* (London) **200**, 269–294.

Mather, G. & West, S. (1993). Evidence for second-order motion detectors. *Vision Research* **33**, 1109–1112.

Newsome, W.T. & Paré, E.B. (1986). MT lesions impair discrimination of direction in a stochastic motion display. *Society of Neuroscience Abstracts* **12**, 1183.

O'Keefe, L.P., Carandini, M., Beusmans, J.M.H. & Movshon, J.A. (1993). MT neuronal responses to 1st- and 2nd-order motion. *Society for Neuroscience Abstracts* **19**, 1283.

O'Keefe, L.P. & Movshon, J.A. (1996). First- and second-order motion processing in superior temporal sulcus of the alert macaque. *Society for Neuroscience Abstracts* **22**, 716.

Orban, G.A., Dupont, P., De Bruyn, B., Vogels, R., Vandenberghe, R. & Mortelmans, L. (1995). A motion area in human visual cortex. *Proceedings of the National Academy of Sciences of the U.S.A.* **92**, 993–997.

Pantle, A. & Picciano, L. (1976). A multistable movement display: Evidence for two separate motion systems in human vision. *Science* **193**, 500–502.

Pantle, A. & Turano, K. (1986). Direct comparisons of apparent motions produced with luminance, contrast-modulated (CM), and texture gratings. *Investigative Ophthalmology and Visual Science* **27**, 141.

Pelli-Robson Contrast Sensitivity Chart (1988). UK: Metropis Ltd.

Petersik, J.T., Hicks, K.I. & Pantle, A.J. (1978). Apparent movement of successively generated subjective figures. *Perception* **7**, 371–383.

Plant, G.T., Laxer, K.D., Barbaro, N.M., Schiffman, J.S. & Nakayama, K. (1993). Impaired visual motion perception in the contralateral hemifield following unilateral posterior cerebral lesions. *Brain* **116**, 1337–1353.

Rademacher, J., Galaburda, A.M., Kennedy, D.N., Filipek, P.A. & Caviness, V.S. (1992). Human cerebral cortex: Localization, parcellation, and morphometry with magnetic resonance imaging. *Journal of Cognitive Neuroscience* **4**, 352–374.

Ramachandran, V.S., Rao, V.M. & Vidyasagar, T.R. (1973). Apparent movement with subjective contours. *Vision Research* **13,** 1399–1401.

Randot Stereotests (1956). Chicago, Illinois: Stereo Optical Company, Inc.

Reichardt, W. (1961). Autocorrelation, a principle for the evaluation of sensory information by the central nervous system. In *Sensory Communication,* ed. Roseblith, W.A., pp. 303–317. New York: Wiley.

Rodman, H.R. & Albright, T.D. (1989). Single-unit analysis of pattern-motion selective properties in the middle temporal visual area (MT). *Experimental Brain Research* **75**, 53–64.

Saiviroporoon, P. (1992). *A computerized instrument for the diagnosis of visual deficits in humans*. M.S. Thesis, Department of Biomedical Engineering, Boston University.

Smith, A.T., Hess, R.F. & Baker, C.L.J. (1994). Direction identification thresholds for second-order motion in central and peripheral vision. *Journal Optical Society of America A* **11**, 506–513.

Sperling, G. (1976). Movement perception in computer-driven visual displays. *Behavioural Research Methods and Instrumentation* **8**, 144–151.

Talairach, J. & Tournoux, P. (1988). *Co-Planar Stereotaxic Atlas of the Human Brain.* New York: Georg Thieme Verlag.

Tootell, R.B.H., Reppas, J.B., Kwong, K.K., Mallach, R., Born, R.T., Brady, T.J., Rosen, B.R. & Belliveau, J.W. (1995). Functional analysis of human MT and related visual cortical areas using magnetic resonance imaging. *Journal of Neuroscience* **15**, 3215–3230.

Turano, K. & Pantle, A. (1989). On the mechanism that encodes the movement of contrast variations: Velocity discrimination. *Vision Research* **29**, 207–221.

Ullman, S. (1979). *The Interpretation of Visual Motion*. Cambridge, Massachusetts: MIT Press.

Vaina, L.M. (1989). Selective impairment of visual motion interpretation following lesions of the right occipito-parietal area in humans. *Biological Cybernetics* **61**, 347–359.

Vaina, L.M., LeMay, M., Bienfang, D.C., Choi, A.Y. & Nakayama, K. (1990*a*). Intact "biological motion" and "structure from motion" perception in a patient with impaired motion mechanisms: A case study. *Visual Neuroscience* **5**, 353–369.

Vaina, L.M., Grzywacz, N.M. & LeMay, M. (1990*b*). Structure from motion with impaired local-speed and global motion-field computations. *Neural Computation* **2**, 420–435.

Vaina, L.M., Grzywacz, N.M. & Kikinis, R. (1994). Segregation of computations underlying perception of motion discontinuity and coherence. *NeuroReport* **5**, 2289–2294.

Vaina, L.M., LeMay, M. & Gryzwacz, N.M. (1993). Deficits of non-Fourier motion perception in a patient with normal performance on short-range motion tasks. *Society for Neuroscience Abstracts* **19**, 1284.

Vaina, L.M., Makris, N., Kennedy, D. & Cowey, A. (1996*a*). The neuroanatomical damage producing selective deficits of first- or second-order motion in stroke patients provides further evidence for separate mechanisms. *NeuroImage* **V3/3**, 360.

Vaina, L.M., Royden, C.S., Bienfang, D.C., Makris, N. & Kennedy, D.(1996*b*). Normal perception of heading in a patient with impaired structure from motion. *Investigative Ophthalmology and Visual Sciences* **37**, 515.

Vaina, L.M. & Cowey, A. (1996). Impairment of the perception of second-order motion but not first-order motion in a patient with unilateral focal brain damage. *Proceedings of the Royal Society B* (London) **263**, 1225–1232.

Vaina, L.M. (1996). Akinetopsia, achromatopsia and blindsight: Recent studies on perception without awareness. *Synthese* **105**, 253–271.

Van Santen, J.P.H. & Sperling, G. (1985). Elaborated Reichardt detectors. *Journal Optical Society of America A* **2**, 300–321.

Victor, J.D. & Conte, M.M. (1990). Spatial organization of nonlinear interactions in form perception. *Vision Research* **31**, 1457–1488.

Warrington, E. & James, M. (1991). *The visual object and space perceptual battery*. Bury St. Edmunds: Thames Valley Test Company.

Watson, A.B. & Ahumada, A.J. (1985). A model of human visual-motion sensing. *Journal Optical Society of America A* **2**, 322–342.

Watson, J.D.G., Meyers, R., Frackowiak, R.S.J., Hajnal, J.V., Woods, R.P. & Mazziotta, J.C. (1993). Area V5 of the human brain: Evidence from a combined study using positron emission tomography and magnetic resonance imaging. *Cerebral Cortex* **3**, 79–94.

Werkhoven, P., Sperling, G. & Chubb, C. (1993). The dimensionality of texture-defined motion: A single channel theory. *Vision Research* **33**(4), 463–486.

Wilson, H.R., Ferrera, V.P. & Yo, C. (1992). A psychophysically motivated model for two-dimensional motion perception. *Visual Neuroscience* **9**, 79–97.

Zeki, S. (1991). Cerebral akinetopsia (visual motion blindness): A review. *Brain* **114**, 811–824.

Zeki, S., Watson, J.D.G., Lueck, C.K., Friston, K.J., Kennard, C. & Frackowiak, R.S.J. (1991). A direct demonstration of functional specialization in human visual cortex. *Journal of Neuroscience* **11**, 641–649.

Zhou, Y.-X. & Baker, C.L.B., Jr. (1993). A processing stream in mammalian visual cortex neurons for non-Fourier responses. *Science* **261**, 98–101.

Zihl, J., von Cramon, D., Mai, N. & Schmid, C. (1991). Disturbance of movement vision after bilateral posterior brain damage. *Brain* **114**, 2235–2252.

Zihl, J., von Cramon, D. & Mai, N. (1983). Selective disturbance of movement vision after bilateral brain damage. *Brain* **106**, 313–340.